

**Seasonal hydrological and nutrient loading forecasts for watersheds over the
Southeastern United States**

Satish Bastola^{1,#} and Vasubandhu Misra^{2,3,4}

¹ School of Civil and Environmental Engineering, Georgia Institute of Technology,
Atlanta, Georgia

² Department of Earth, Ocean and Atmospheric Sciences, Florida State University,
Tallahassee, Florida

³ Florida Climate Institute, Florida State University, Tallahassee, Florida

⁴ Center for Ocean-Atmospheric Prediction Studies, Florida State University,
Tallahassee, Florida

Corresponding author email: Satish.bastola@ce.gatech.edu

18

19 **Abstract**

20 We show useful seasonal deterministic and probabilistic prediction skill of
21 streamflow and nutrient loading over watersheds in the Southeastern United States
22 (SEUS) for the winter and spring seasons. The study accounts for forecast
23 uncertainties stemming from the meteorological forcing and hydrological model
24 uncertainty. Multi-model estimation from three hydrological models, each forced
25 with an ensemble of forcing derived by matching observed analogues of forecasted
26 quartile rainfall anomalies from a seasonal climate forecast is used. The attained
27 useful hydrological prediction skill is despite the climate model overestimating
28 rainfall by over 23% over these SEUS watersheds in December-May period. The
29 prediction skill in the month of April-and May is deteriorated as compared to the
30 period from December-March (zero lead forecast).

31 A nutrient streamflow rating curve is developed using a log-linear tool for this
32 purpose. The, skill in prediction of seasonal nutrient loading is nearly identical to the skill
33 in predicting the seasonal streamflow.

34

35 **Keywords:** Rainfall-runoff model, Seasonal Hydrologic Forecasting, Southeastern
36 United States, Water Quality, Seasonal Predictability

37 **Software availability**

38 Name: Catchment hydrological model (subroutine written in FORTRAN)

39 Availability: Available upon request from the authors.

40

41 **1. Introduction**

42 The Southeastern United States (SEUS) region receives considerable amounts of
43 rainfall ranging spatially between 30 and 100 inches annually relative to the rest of the
44 United States (<http://www.nc-climate.ncsu.edu/edu/k12/.SEPrecip>). However, the water
45 sector remains vulnerable because the region is exposed to significant climate variability
46 including relatively frequent climate and weather extremes like droughts and landfalling
47 tropical cyclones. There are several studies, which have suggested the benefit of
48 streamflow predictions in managing and regulating water resources (e.g., Broad 2007;
49 Yao and Gergakakos 2001; Obeysekera et al. 1999). For example, Obeysekera et al.
50 (1999) noted the benefit of long-range hydrological forecasts for the complex water
51 management system in South Florida, consisting of large reservoirs, lakes, and water
52 regulating structures. However, Bolson et al. (2013) reported that only about 25% of the
53 water managers use seasonal climate forecasts. Many studies have attributed this
54 infrequent use to lack of awareness and difficulty in understanding, trusting, and applying
55 the forecasts (e.g., Carbone and Dow 2005; Pagano et al. 2001).

56

57 The reliability of streamflow forecasts depends on, among other factors, the
58 fidelity of the climate forecast, the reliability of the hydrological models, and the quality
59 of the initial hydrologic conditions used. Over the years considerable progress has been
60 made in improving dynamical seasonal prediction (Kumar et al. 1996; Krishnamurti et al.
61 1999; Palmer et al. 2004; Zhang et al. 2007; Yang et al. 2009; Kirtman and Min 2009;
62 Saha et al. 2010; Gent et al. 2011; Misra et al. 2013; Li and Misra 2013; Kirtman et al.
63 2014). Furthermore, Maurer et al. (2004) claim that a better understanding of the

64 teleconnections between large-scale climate features and the hydroclimatology of the
65 region can improve the streamflow forecast for longer lead times. In the SEUS, the El
66 Niño–Southern Oscillation (ENSO) teleconnections are relatively strong, especially
67 during the boreal winter and spring seasons (Ropelewski and Halpert 1987, 1986; Kiladis
68 and Diaz 1989). In a typical El Niño (La Niña) year, the SEUS experiences a cold and
69 wet (warm and dry) winter season. Such robust teleconnections provide an opportunity to
70 improve water resource management at the seasonal to interannual time scales.

71

72 To provide predictions of streamflow at long lead times, empirical methods (e.g.,
73 multiple linear regression) have long been used in the United States (e.g., Rosenberg et
74 al. 2011; Pagano et al. 2009). These methods use initial conditions and information on
75 future climate condition as predictors. However, ensemble streamflow prediction (ESP;
76 Day 1985) is also being widely considered as an alternative to multiple linear regressions
77 (e.g., Connelly et al. 1999; Franz et al. 2003; Wood et al. 2005; Wood and Schaake 2008;
78 Bohn et al. 2010) and is adopted in this study as well. In the ESP method, multiple
79 realizations of future streamflow are simulated. These realizations are usually generated
80 by independently running multiple calibrated hydrological models forced with multiple
81 realizations of surface meteorological forcing (discussed further in section 3). ESP has
82 some notable advantages over empirical models: ESP makes predictions on physical and
83 conceptual basis, provides an estimate of the forecast uncertainty and offers flexibility in
84 using forcing data from different sources (e.g., climate model, subjective climate
85 outlooks).

86

87 A study from NRC (2000) recognized that nutrient loading is the main cause of
88 eutrophication of freshwater bodies and coastal estuaries. The stream nutrient loads
89 depend upon, among other factors, precipitation, temperature, soil, geology, nutrient fate
90 and transport; however, urban and agriculture landscape have the greatest impact (Preston
91 et al. 2011). These sources of nutrient loading can be broadly classified as point source
92 and nonpoint source. Managing and controlling these excessive nutrients relies on
93 instream nutrient concentration data that are only sparsely available. Therefore,
94 mathematical models are widely used in aiding local nutrient management and control. A
95 broad array of models ranging from empirical models such as simple export coefficient to
96 physically based nutrient modeling tools are available to estimate pollution and identify
97 the sources at watershed scale (Shrestha et al. 2008; Arnold et al. 1994; EPA 1987; Smith
98 et al. 1997; Ambrose et al. 1981; Johanson et al. 1981). Most of these studies show strong
99 empirical evidence that streamflow is the single most important variable for estimating
100 the pollution load of namely total nitrogen and total phosphorous. These nutrients are
101 responsible for the impairment of many inland waters as well as coastal bays. Excessive
102 amounts of these nutrients promote profuse algae growth, resulting in unhealthy inland
103 and coastal waters.

104

105 Studying over 6300 water bodies located in Florida using a range of chemical and
106 biological parameters, the Florida Department of Environmental Protection (FDEP) in the
107 year 2008 found impairment in 28% of the stream miles, 25% of lake acres, and 59% of
108 square miles of estuaries. The FDEP has recently imposed a numeric nutrient criteria
109 water quality standard specifically for nitrogen and phosphorous (FDEP 2012). In

110 response to adoption of such water quality standards, water quality credit trading is likely
111 to emerge as one of the policy tools to preserve water quality in a cost-effective manner
112 [e.g., pilot water quality credit trading program for the lower St. Johns River (FDEP
113 2010); establishment of pollutant trading policy advisory committee to assist FDEP in
114 developing a pollutant trading program (FDEP 2006)]. Nutrient trading is especially
115 beneficial in avoiding impairment of waterways and water bodies if the cost involved in
116 controlling pollutants from the various sources within a watershed is considerably
117 different and water quality goals are firmly established.

118 In this study, we analyze a relatively large set of retrospective seasonal
119 streamflow forecast experiments for the boreal winter and spring months for watersheds
120 in the SEUS using the seasonal climate forecasts produced by the Florida Climate
121 Institute (FCI) of the Florida State University (FSU; Misra et al. 2013 and Li and Misra
122 2013). Li and Misra (2013) demonstrated that the FCI-FSU Seasonal Hindcasts at 50km
123 grid resolution (FISH50) seasonal mean temperature and precipitation has comparable
124 skill for boreal winter and spring relative to the operational models of the National Multi-
125 Model Ensemble (NMME; Kirtman et al. 2014). FISH50 also offers the highest spatial
126 resolution among the existing seasonal climate hindcast data sources (e.g., NMME).
127 Therefore, through this study, we aim to explore the utility of FISH50 for seasonal
128 hydrologic forecasts. We follow up this analysis with estimations of retrospective
129 seasonal forecasts of nutrient loading, which are based on the empirical nutrient
130 streamflow rating curve and the predicted streamflow. We consider only total nitrogen
131 and total phosphorous as they are widely regarded as predictors of stream-water quality
132 (USEPA 2006).

133 It may be noted that this is first of such attempt to apply retrospective multi-model
134 seasonal hydrological forecast framework for the boreal winter and spring seasons over
135 these relatively small 28 SEUS watersheds.

136

137 **2. Study region and data**

138 In this study, a total of 28 watersheds from the Model Parameter Estimation
139 Experiment (MOPEX; Schaake et al. 2006) is selected, which follows from our previous
140 work on the summer seasonal forecasts (Bastola et al., 2013). These watersheds are
141 chosen because they are minimally affected by water management (Schaake et al. 2006).
142 The characteristics of the selected watershed is shown in Table 1.

143 FISH50 is initialized in late November through early December of each year and
144 integrated through May of the subsequent year for 1982–2008. Each of the seasonal
145 hindcasts of FISH50 has a total of six ensemble members, which are generated by
146 perturbing the initial conditions of the atmosphere (Li and Misra 2013). The data from
147 FISH50 is available at daily time scale from December through May of the following
148 year. It may be mentioned that in this forecast framework of FISH50 December-January-
149 February (DJF) seasonal mean is at zero lead while the March-April-May (MAM)
150 seasonal mean will be at one season lead. We use the unified daily US precipitation
151 analysis of the Climate Prediction Center (CPC; Higgins et al. 2000), available at 0.25°
152 grid resolution and from 1948 onward, as the observed rainfall.

153

154 **3. Hydrological model forcing**

155 Bias correction and the stochastic method are two common approaches that are
156 widely used to bridge the spatial resolution gap that exists between the hydrological and
157 the climate models. To correct for systematic biases in rainfall forecasts, the quantile-
158 based bias correction method has been used extensively in hydrological applications (e.g.,
159 Li et al. 2010; Wood et al. 2004). The stochastic method is based on resampling from
160 historical observations (e.g., the Schaake shuffle in Clark et al. 2004). The resampling
161 from analogue years is based on categorical climate forecasts (e.g., forecasts based on
162 tercile or quartile categories of seasonal precipitation anomalies). It preserves the various
163 moments of a time series (e.g., Efron 1979).

164 In this study, bias correction based on resampling from historical observation is
165 used to circumvent the issue of bias in FISH50. The resampling method to generate a
166 conditioned daily sequence of meteorological forcing for the semi-distributed
167 hydrological models (which includes sub basin average rainfall, temperature, and
168 evapotranspiration) is as follows (see Bastola et al. (2014) for further details):

- 169 1. Based on 6-month averaged (Dec-May) forecast rainfall, derive the quartile
170 category for each year for a given watershed,
- 171 2. Sample 10 sets of model forcing for hydrological model (a block of 6 month (Dec-
172 May) from historical observation of weather data that has same quartile category as
173 that of forecast seasonal mean (December-May) rainfall.
- 174 3. Repeat step 1 and 2 for each of the six-ensemble member of the FISH50.

175 This procedure generates 10 resamples for each ensemble member and then propagates
176 them through three hydrological models. We thus obtain 180 (=6 ensemble members

177 of FISH50 x 10 observed resamples per ensemble member of FISH50 x 3 hydrological
178 models) estimates of streamflow for each watershed per season.

179

180 In this study, the FISH50 seasonal categorical rainfall forecast (based on quartile
181 rainfall categories) is used to sample from the observed analogue. The resampling of the
182 past observations is done several (10) times per ensemble member of FISH50 using the
183 method of block resampling without replacement (Prudhomme and Davies 2009). Here
184 we define a block as six months of continuous daily rainfall. Though plausible,
185 resampling with a block size of a month or three months is likely to affect the seasonal
186 structure and to introduce biases (Prudhomme and Davies 2009). Furthermore, ten
187 resamples per ensemble member of FISH50 enables us to attain a good sample of the
188 observed near analogues of the forecasted meteorological forcing to make a robust
189 probabilistic streamflow forecast (Fig. 1). It may also be mentioned that this resampling
190 from historical observed data also temporally disaggregates the seasonal forecast total
191 into daily values. In this way, the resampling procedure generates multiple time series of
192 rainfall from a historical record. In addition, semi-lumped [parameters are lumped over
193 the whole river basin with spatial variation in the model (meteorological) forcing]
194 hydrological models are implemented for the hydrological predictions conducted in this
195 study. Therefore, development of a spatially coherent sub-basin average rainfall field is
196 essential. In this context, resampling from historical observation allows development of
197 spatially coherent sub-basin average rainfall (see Bastola et al., 2013).

198 In this study, we compare the performance of the hydrological forecasts between
199 those that use the FISH50 meteorological forcing directly without any bias correction

200 (named hereafter as FISH50) and those that use the resampled observations using quartile
201 categories of seasonal mean rainfall from FISH50 (FISH50_Resamp). Evaluation of
202 output from environmental modeling using suitable performance measure is essential
203 before they can be confidently used for their practical application. Hydrologists
204 fundamentally use qualitative (visual) and objective criteria to judge the reliability of
205 output from hydrological simulation. The quantitative criteria most widely used is the
206 efficiency criteria derived from summation of error term normalized by the variability in
207 observation data (Beven and Binley 1992, Bennett et al., 2013). Two commonly used
208 residual methods namely, persistence index and Nash-Sutcliffe Model efficiency (Table
209 6 of Bennett et al., 2013) is used to evaluate the seasonal hydrological forecasts in this
210 study. Furthermore, receiver operating characteristics curves (ROC) is used to evaluate
211 the probabilistic forecast, again one of the commonly used probabilistic skill metrics
212 (Wilks 2001).

213

214 **4. Experiment design**

215 *i) Hydrological forecasts*

216 In this study, the seasonal hydrological forecast experiment, which is carried out
217 using the FISH50 data for 20 years (1982–2001), is based on ESP methodology (Fig. 1).
218 The FISH50 dataset is available for a six-month period from December through May of
219 the subsequent year. The initial conditions for the hydrological models are obtained by
220 forcing the hydrological models with the observed meteorological forcing up to the start
221 (or initial) time of the forecast (e.g., Wood and Lettenmaier 2006).

222 Though there is consensus on the importance of uncertainty analysis in
223 hydrological modeling and subsequently on water resource planning and management,
224 there is an intense debate on the framework needed to quantify uncertainty (e.g., Beven et
225 al. 2012; Clark et al. 2012; Kuczera, 1997; Beven and Binley 1992; Duan et al. 1992).
226 The discussion and implementation of different methods is beyond the scope of this
227 study. In this study, we account for the uncertainty of the hydrological forecasts arising
228 from model uncertainty and meteorological forcing (Fig. 1). The latter form of
229 (meteorological) uncertainty is estimated from the 60 ensemble members generated from
230 10 observed resamples for each of the 6 ensemble members of FISH50 per season (see
231 Section 3). The model uncertainty is accounted for by combining the retrospective
232 predictions derived from three conceptual rainfall-runoff (RR) model structures and their
233 behavioral model parameters. The concept of combining the output from multiple models
234 is growing in the field of climate and environmental modelling. Combining the output
235 from multiple models allows for the characterization of structural uncertainties in the
236 models. Furthermore, multimodel approach may also lead to more skillful
237 simulation/prediction as it accounts for model uncertainty (e.g., Krishnamurti et al., 1999,
238 Georgakakos et al., 2004; Kirtman and Min 2009).

239

240 The three RR models used in this study are the Hydrologic MODel (HyMOD;
241 Boyle 2001), the Nedbør-Afstrømnings Model (NAM; Madsen 2000), and the tank model
242 (Sugawara 1995). All three hydrological models are implemented as semi-lumped and are
243 conceptual in the sense that model calibration is essential for the estimation of model

244 parameters. The HyMOD, NAM, and tank have 6, 10, and 16 spatially lumped
245 parameters, respectively.

246

247 Hydrological modeling literature, in general, agrees that large combinations of
248 parameters can result in equally acceptable model simulations (Beven 2006). Therefore,
249 we implement a multimodel and multiparameter approach using the generalized
250 likelihood uncertainty estimation method (GLUE; Beven and Binley 1992) to account for
251 uncertainty in hydrological simulation. In GLUE, the ensemble simulation is obtained by
252 weighting the model prediction with model's likelihood measure (Beven and Binley,
253 1992).

254 This study builds upon our previous study (Bastola and Misra 2013), which
255 focused on calibration of 28 MOPEX watersheds of the SEUS for the three selected
256 hydrological models. The authors calibrated the three conceptual models for the period
257 1948–1968 using CPC rainfall data. The hydrological models were then validated for the
258 period of 1969–1979. The performance of individual model for the entire watershed is
259 measured in terms of the three widely used model performance criteria, namely, the Nash
260 Sutcliffe efficiency index (NSE), Count Efficiency (CE), which is estimated as the
261 percentage of observation included within the Prediction interval (PI) and width of
262 prediction interval. For calibration of each of the three hydrological models, they were
263 used in simulating independently, for each watershed, with 20,000 set of randomly
264 generated model parameters from a uniform distribution. From among these huge set of
265 simulations, only behavioural set of model parameters that result in a value of NSE
266 greater than 0.5 were retained. The model calibration attempt also revealed that the

267 combination of output from the different models improved the reliability and
268 performance of the simulation (not shown). Further details on model calibration and
269 validation can be found in Bastola and Misra (2013).

270

271

272 *ii) Simulation of instream water quality*

273 Fernandez et al. (2006) and Shrestha et al. (2008) used a multiple linear
274 regression (log-linear model) to model nutrient loading rate. They reported that a simple
275 log-linear model performs reasonably well in estimating nutrient loadings. A regression
276 model such as load estimator (LOADEST) is traditionally used to predict water quality
277 constituent concentration by linearly relating it with the natural log of streamflow, time,
278 and season (Runkel et al., 2004). Another such regression-based model for modeling
279 nutrient loading rate is the weighted regression on time, discharge and season (WRTDS;
280 Hirsch et al. 2010). More recently, Oh and Sankarasubramanian (2012) looked at the
281 potential application of seasonal forecasts of nutrient loading on a few SEUS watersheds
282 by applying seasonal climate forecasts and the LOADEST. They looked at the variability
283 of the nutrient loadings associated with seasonal climate variability in watersheds that are
284 minimally disturbed. Oh and Sankarasubramanian (2012) conditioned their nutrient
285 prediction on the basis of precipitation as they found a strong correlation between
286 simulated loading and precipitation. They first developed the nutrient loading rating
287 curve by relating nutrient loads with observed streamflow. Then they used empirical
288 orthogonal function and canonical correlation analysis based on simulated loading and
289 the gridded winter precipitation to develop a low-level model to predict loadings for each

290 watershed on the basis of climate forecasts from a climate model. Their study
291 demonstrated useful prediction skills of the winter season total nitrogen behavior in the
292 coastal watersheds of the SEUS.

293 The streamflow is selected as the predictand as it has been found to be the most
294 important variable in predicting nutrients. Except for the two watersheds in south Florida,
295 all of the watersheds included in this study of nutrient loading forecasts were included in
296 Oh and Sankarasubramanian (2012) study. Among the 28 watersheds used in this study,
297 only seven of these SEUS watersheds have the data on nutrient load. Therefore, water
298 quality forecast is shown only for these seven SEUS watersheds.

299

300 Because nutrient measurements are only sparsely available, load estimation using
301 regression-based models has been widely explored for watershed management, especially
302 for watershed planning pollution control (Shrestha et al. 2008). LOADEST, a tool for the
303 estimation of nutrient load based on a number of explanatory variables (e.g., streamflow,
304 decimal time, concentration, etc.) is used in this study. Further details on the calibration
305 and load estimation procedure are found in Runkel et al. (2004). Unlike the watersheds
306 in Oh and Sankarasubramanian (2012), all watersheds included in the nutrient loading
307 forecast experiment are calibrated in this study.

$$\begin{aligned} \ln(L) &= a_0 + a_1 \ln(O) + a_2 \sin(2\pi(T - T')) + a_3 \cos(2\pi(T - T')) & 1 \\ \ln(O) &= \ln(Q) - \ln(Q)' & 2 \end{aligned}$$

309 where, L is the load in kg per day; Q is the streamflow in cubic feet per sec; $a_0, a_1, a_2, a_3,$
310 are the regression coefficients, T is the time measured in years (decimal) and T' is the
311 coefficient that defines the center of decimal time; $\ln(Q)'$ is the coefficient that defines
312 the center of the streamflow. The explanatory variable $\ln(O)$ is centered to avoid co-

313 linearity. Both T' and $\ln(Q)'$ are the coefficient estimated from observed data, i.e., load
314 and streamflow data from the U.S. Geological Survey national stream water-quality
315 monitoring networks (<http://pubs.usgs.gov/dds/wqn96cd/html/wqn/wq/region03.htm>)
316 (WQN). The retrospective seasonal forecast of total nitrogen and phosphorous is
317 computed from (1 & 2). We explored numerous model structure (model option) available
318 in LOADTEST. Amongst all available choices, the option 4 (a four-parameter log linear
319 model) of LOADTEST was selected based on its relative performance measured in terms
320 of R^2 . The calibrated parameters and performance of model for the selected watersheds
321 is shown in Table 2.

322

323 **5. Results and discussion**

324 Following Bastola et al. (2013) we will compare the seasonal forecast skill to
325 climatology and one-year lag (persistence) forecast. Furthermore, we will use the Nash
326 Sutcliffe Efficiency (NSE) and Area under the Relative Operating Characteristic Curve
327 (AROC; Marzban 2004) as our deterministic and probabilistic metrics for forecast skill
328 analysis respectively. The NSE derived from the normalized form of root mean square
329 error (2) is used to evaluate the skill of FISH50 with respect to two simple reference
330 forecasts: (a) a climatological forecasts (NSE; Eq 3) and (b) a one-year lag (persistence)
331 forecast (Persistence; Eq 4). The NSE and Persistence are both alternate form of root
332 mean square error. NSE (which range from $-\infty$ to 1) is the normalized root mean square
333 error, which measures the relative magnitude of residual variance to observed variance
334 thereby reflecting how well the simulated value fits observations. An NSE of 1 reflects
335 perfect model and negative value indicates that the skill of the model is worse than using

336 climatology. NSE is one of the most widely used and recommended performance
337 measures for evaluating hydrological predictions and simulations.

338 The persistence model efficiency is also a normalized statistic as NSE, but the sum of the
339 square of the error is normalized differently (i.e. with respect to one lag forecast). Both
340 NSE and persistence are however biased towards large data values (or high flow period).
341 However these skill metrics also penalize the prediction if they underestimate the high
342 flow period.

343

$$NSE = 1 - \frac{\sum_{i=1}^n (Q_{obs,i} - Q_{sim,i})^2}{\sum_{i=1}^n (Q_{obs,i} - \bar{Q})^2} \quad 3$$

344

$$Persistence = 1 - \frac{\sum_{i=1}^n (Q_{obs,i} - Q_{sim,i})^2}{\sum_{i=1}^n (Q_{obs,i} - Q_{obs,i-1})^2} \quad 4$$

345 The Relative (or sometimes referred as Receiver) Operating Characteristic Curve
346 (ROC) describes the relation between the probability of correct (hit rate) and incorrect
347 (false alarm rate) forecasts from a given model. In ROC, models ability to correctly
348 predict the event is plotted versus models ability to exclude a condition correctly. The
349 area under the curve reflects the performance of the predictive models.

350 Unlike NSE, it takes into account the forecast uncertainty as described by the forecast
351 spread of the individual ensemble members. In the adopted methodology of using
352 resampled historical observations for forcing the multiple hydrological models, we
353 generate a relatively large number of ensemble members (=180; see Section 3) per
354 season, which provides a robust measure of AROC for the streamflow predictions. It may
355 be noted that the value of AROC < 0.5 suggests that the skill is no better than observed
356 climatology.

357

358 *i) Deterministic skill analysis*

359 In this section, ensemble spreads of the predictions are ignored, and skills are
360 evaluated on the basis of the ensemble mean. The experiment design explained earlier
361 produces an ensemble of predicted flows from the FISH50 ensemble and the multiple
362 calibrated hydrological models (Fig. 1). Hydrological model output simulated with the
363 observed CPC rainfall data is used as a control, or truth, to verify the fidelity of the
364 hydrological predictions.

365 For the 28 SEUS watersheds included in this study, the spatially averaged daily
366 rainfall from December through May from FISH50 is significantly higher compared to
367 rainfall from CPC (Fig. 2), the reference rainfall dataset. Over most of the watersheds,
368 FISH50 overestimates observed rainfall by nearly 23%. Such a high bias may have a
369 greater impact on the SEUS watersheds characterized by high precipitation elasticity of
370 streamflow (e.g., Sankarasubramanian et al. 2001).

371 Fig. 3 shows that the bias (i.e., the volume error in simulated flow associated with
372 the FISH50 forcing), which is high for some watersheds, is significantly reduced with the
373 use of resampled observations (FISH50_Resamp). Figure 4 shows climatological
374 streamflow only for the selected six watersheds that broadly span our study region of the
375 SEUS. The raw FISH50 forcing data produces significant bias in the seasonal cycle of the
376 streamflow over the majority of the watersheds shown in Fig. 4. The resampling from
377 historical observations based on analogues of the forecasted quartile rainfall category of
378 the December–May season from FISH50 seems to ameliorate some of this bias in the
379 seasonal cycle relative to the control flow (Fig. 4).

380

381 Fig. 5 shows the normalized root mean square errors of the ensemble average
382 streamflow based on two-reference forecasts: the climatological (the NSE) and the lag
383 one-year forecast [or persistent forecast, wherein the observed flow anomalies from the
384 previous year are continued through the following year; persistence efficiency measure
385 (PEM)]. The predicted flow forced with raw FISH50 and FISH50_Resamp shows some
386 skill against both reference forecasts. Skills, however, tend to decrease with lead time.

387

388 *ii) Probabilistic skill analysis*

389 It is prudent to examine the probabilistic skill of these forecasts given the non-
390 deterministic nature of these seasonal forecasts (Palmer et al. 2000). The probabilistic
391 skill score (as measured by AROC) of FISH50 shows some skill in discriminating
392 different (quartile) categories of rainfall. The FISH50 forecasted monthly mean rainfall
393 shows superior skill than corresponding climatology on 27, 19, 12, and 11 watersheds for
394 very wet, wet, dry, and very dry rainfall categories respectively (Fig. 6). In Fig. 6 each
395 bubble represents an AROC value greater than 0.5 for that watershed, and the size of the
396 bubble indicates a relative value of the AROC that is larger than 0.5. The watersheds in
397 Florida, especially the St. Johns and the Peace River, show skill over the climatological
398 forecast in the wet and very wet categories (Fig. 6). Similarly, on the basis of the average
399 value of AROC across watersheds, the very wet and wet categories are more skillful than
400 the dry and very dry rainfall categories (Fig. 6). In addition, most of the watersheds in
401 Georgia and Alabama also show skill in the very wet quartile (Fig. 6).

402

403 The probabilistic skill of the hydrological predictions derived from FISH50 is
404 examined, given the skill of FISH50 in discriminating the different quartile categories of
405 the seasonal rainfall. The AROC for streamflow is calculated as the probabilistic measure
406 to evaluate the experimental hydrological forecast using all 180 realizations per season
407 for each of the 28 watersheds of the SEUS. Fig. 7 shows that on average, very wet and
408 wet categories show more skill (on the basis of the number of watersheds with AROC
409 values > 0.5) compared to the other two quartile categories (i.e., very dry and dry). The
410 AROC values for the forecasted streamflow for each of the 28 watersheds and each
411 month of the season for all the four quartiles are shown in Figs. 8 and 9. The results
412 shown in these figures are consistent with similar analysis of FISH50 precipitation (Fig.
413 6), which shows that the very wet and wet quartile precipitation categories have higher
414 skill than the other two quartile categories. In other words, the results suggest that for the
415 majority of the SEUS watersheds, the streamflow is sensitive to the quality of the
416 precipitation forecasts. In comparison to the FISH50 summer and fall seasonal
417 hydrological forecasts (Bastola et al., 2013), the winter and spring seasons in Fig. 7 show
418 significantly higher skill.

419

420 *iii) Skill of seasonal nutrient loading simulation*

421 It is expected that the skill in streamflow will be translated into skill in predicting
422 nutrient loading as the log-linear model (equation 1) is used to predict the nutrient load
423 from the flow and the day of the year, The AROC value for the seven watersheds for
424 which nutrient loading data are available is shown for only two categories, i.e., very wet
425 and very dry quartiles (Figs. 10 and 11). As the skills of the nutrient loading forecasts are

426 identical to the skills in seasonal streamflow prediction, the AROC values for the middle
427 quartiles are not shown. Any differences between the skills in streamflow and nutrient
428 loading can be attributed to the performance of the log linear model during calibration. In
429 Figs. 10 and 11 the skills for both total Nitrogen and total Phosphorous loading for both
430 extreme quartile categories are nearly similar to their corresponding streamflow
431 prediction skills. However, it is apparent from comparing Figs. 10 and 11 that there is
432 more skill in the seven watersheds in forecasting monthly nutrient loadings for the very
433 wet quartile (Fig. 10) than for the very dry quartile (Fig. 11), which follows from similar
434 features observed in streamflows (Figs. 8 and 9). Only seven watersheds which had
435 required water quality data were only considered compared to the 28 watersheds used to
436 evaluate the seasonal predictability of stream flow. This skill in the seasonal forecast of
437 the monthly nutrient loading can be exploited in revising the total maximum daily load
438 that waterways can carry without being impaired. In Florida, the FDEP has imposed a
439 numeric nutrient criteria water quality standard specifically for nitrogen and
440 phosphorous. The skill in seasonal prediction of nutrient loading is likely to promote
441 nutrient trading, especially since nutrient trading has been recently proposed as a major
442 policy to address impairment of waterways and water bodies in Florida.

443 The simulation of nutrient loading is based on the forecasted streamflow and a
444 relationship between nutrient load and streamflow calibrated from historical observed
445 streamflow and nutrient loading data. The nutrient prediction model only accounts for the
446 influence of the variability in rainfall and streamflow on nutrient dynamics and does not
447 account for the influence of land use explicitly in the dynamics of nutrient.

448

449 **7. Conclusion**

450 The seasonal climate retrospective forecasts for the boreal winter and spring
451 seasons of FISH50 are evaluated over the SEUS region in simulating streamflow across
452 28 watersheds and nutrient loading for a small subset (6) of these watersheds. A seasonal
453 hydrological forecast experiment is designed on the basis of an ESP framework, forced
454 with FISH50 meteorological forcing. Three semi-distributed hydrological models are
455 adopted for this study. The experiment setup allows for sampling the hydrological model
456 uncertainty and the meteorological forcing uncertainty. The first uncertainty is handled
457 by using a multimodel approach to predict the streamflow. It is found that over the 28
458 watersheds, FISH50 overestimated the winter and spring rainfall total by nearly 23%.
459 Therefore, some form of bias correction of rainfall is essential for the application of
460 FISH50 in hydrology. The selected watersheds are characterized by high precipitation
461 elasticity of streamflow, which makes bias correction of forecasted rainfall essential.
462 Bias correction of rainfall from FISH50 is accomplished by resampling the observed
463 seasonal (December–May) historical record with quartile categories similar to those of
464 the FISH50 forecast, which also serve in sampling the uncertainty of the meteorological
465 forcing to the hydrological models.

466 The experimental setup, therefore, entails 180 ensemble members per season,
467 which includes three hydrological models and 10 samples of observed analogues of
468 meteorological forcing per ensemble member of FISH50 (which has 6 ensemble
469 members per season).

470 In this study, we examine both the deterministic and the probabilistic skill
471 measures of the meteorological forcing, the predicted streamflow, and the nutrient

472 loading. The former skill measure entails examining the ensemble mean, which ignores
473 the ensemble spread and the forecast uncertainty therein, whereas the latter uses the
474 forecast from all ensemble members.

475 The seasonal hydrologic forecasts based on ensemble average show superior skill
476 relative to the climatological and lag one-year forecast based on the measures of the NSE.
477 However, these prediction skills show a clear decrease with lead time. In this study, we
478 also use AROC value as a measure of the probabilistic skill of the forecast. The
479 probabilistic skill score of the predicted streamflow is encouraging for the selected
480 watersheds. Especially for the top and middle top quartiles (i.e., the very wet and wet
481 quartile categories), the FISH50 rainfall product for December–May shows
482 comparatively higher skill than the climatology over most of the SEUS watersheds.

483 For the subset of seven watersheds selected for studying nutrient loading, the log-
484 linear model appears to perform well in modeling the total nitrogen and total
485 phosphorous load. The strong relationship between nutrient loading and streamflow
486 implies that forecast skill in winter streamflow can be potentially exploited in predicting
487 the nutrient load. This advance information on nutrient loading based on seasonal climate
488 forecasts will prove to be essential for maintaining the water quality standards in
489 waterways and water bodies by helping watershed managers plan the total maximum
490 daily load for the season and promote water quality trading.

491

492 **Acknowledgements**

493 We acknowledge Kathy Fearon of COAPS for help with editing this manuscript. This
494 work was supported by grants from NOAA (NA12OAR4310078, NA10OAR4310215,

495 NA11OAR4310110) and USGS G13AC00408. All computations for integration of the
496 seasonal climate model (FISH50) used in this paper were done on the computational
497 resources provided by the Extreme Science and Engineering Discovery Environment
498 (XSEDE) under TG-ATM120017 and TG-ATM120010.
499

500 **References**

501

502 Ambrose, R.B., Wool, T.A., Martin, J.L., Connolly, J.P., Schanz, R.W., 1981: WASP4: A
503 hydrodynamic and water quality model—Model Theory. In: User's Manual and
504 Programmer's Guide unknown:book, US-EPA, Athens,GA.

505 Arnold, J., A. Williams, R. Srinivasan, B. King, and A. Griggs. 1994: SWAT, soil and
506 water assessment tool. Temple, TX 76502. ARS, USDA.

507 Bastola, S. and Misra, V. 2013: Evaluation of dynamically downscaled reanalysis
508 precipitation data for hydrological application. Hydrol. process. doi:
509 10.1002/hyp.9734

510 Bastola, S., Misra, V., Li, H 2013: Seasonal hydrological forecasts for watersheds over
511 the Southeastern United States for boreal summer and fall seasons. Earth
512 Interactions, 17(25), 1-22, doi:10.1175/2013EI000519.1.

513 Bennett, N.D., Croke, B.F.W., Guariso, G., Guillaume, J.H.A., Hamilton, S.H., Jakeman,
514 A.J., Marsili-Libelli, S., Newham, L.T.H., Norton, J.P., Perrin, C., Pierce, S.A.,
515 Robson, B., Seppelt, R., Voinov, A.A., Fath, B.D. and Andreassian,
516 V. (2013) Characterising performance of environmental models. In:
517 Environmental modelling and software, 40 (2013) pp. 1-20.

518 Beven, K. and Binley, A. 1992: The future of distributed models: model calibration and
519 uncertainty prediction. Hydrol. process. 6: 279-298.

520 Beven, K., P. Smith, I. Westerberg, and J. Freer. 2012: Comment on “Pursuing the
521 method of multiple working hypotheses for hydrological modeling” by P. Clark
522 et al., Water resour res. 48, W11801, doi:10.1029/2012WR012282.

523 Beven K. 2006: A manifesto for the equifinality thesis. *J. Hydrol.* 320:18–36.
524 doi:10.1016/j.jhydrol.2005.07.007.

525 Bohn, T. J., M. Y. Sonessa, and D. P. Lettenmaier. 2010: Seasonal hydrologic
526 forecasting: Do multimodel ensemble averages always yield improvements in
527 forecast skill? *J. Hydrometeor.* 11, 1358–1372.

528 Bolson, J., C. Martinez, N. Breuer, P. Srivastava, and P. Knox, 2013: Climate
529 information use among Southeast US water managers: An Assessment of
530 Opportunities. *Reg Environ Change*. In press.

531 Boyle, D. 2001: Multicriteria calibration of hydrological models. PhD dissertation.
532 Tucson, AZ: Department of Hydrology and Water Resources, University of
533 Arizona; 2001.

534 Broad, K., Pfaff, A., Taddei, R., Sankarasubramanian, A., Lall, U., de Assis de Souza
535 Filho, F. 2007: Climate, stream flow prediction and water management in
536 northeast Brazil: societal trends and forecast value. *Climatic Change.* 84: 217–
537 239.

538 Carbone, G. J., and K. Dow, 2005: Water resource management and drought forecasts in
539 South Carolina. *J Am Water Resour As.* 41: 145–155.

540 Clark, M. P., D. Kavetski, and F. Fenicia. 2012: Reply to comment by K. Beven et al. on
541 “Pursuing the method of multiple working hypotheses for hydrological
542 modeling”, *Water resour res.* 48, W11802, doi:10.1029/2012WR012547.

543 Clark, M. P., Gangopadhyay, S., Brandon, D., Werner, K., Hay, L., Rajagopalan, B. and
544 Yates, D. 2004: A resampling procedure for generating conditioned daily weather
545 sequences, *Water resour res.* 40, W04304, doi:10.1029/2003WR002747.

546 Connelly, B. A., D. T. Braatz, J. B. Halquist, M. M. DeWeese, L. Larson, and J. J.
547 Ingram. 1999: Advanced hydrologic prediction system. *J Geophys Res.* 104(D16):
548 19655–19660.

549 Day, G.N. 1985: Extended Streamflow Forecasting Using NWSRFS. *J of Water Res Pl-*
550 *ASCE*, 111(2): 157-170. doi: <http://dx.doi.org/10.1175/JCLI3812.1>

551 Dai, Aiguo, 2006: Precipitation Characteristics in Eighteen Coupled Climate Models. *J.*
552 *Climate*, 19, 4605–4630. doi: <http://dx.doi.org/10.1175/JCLI3884.1>

553 Duan, Q., Sorooshian, S., and Gupta, V.K. 1992: Effective and efficient global
554 optimization for conceptual rainfall-runoff models. *Water resour res.* 28(4):
555 1015– 1031.

556 Efron, B. 1979: Bootstrap methods: Another look at the jackknife, *Ann. Stat.*, 7: 1–26.

557 EPA, 1987: The Enhanced Stream Water Quality Models QUAL2E and QUAL2E-
558 UNCAS: Document and User’s Manual. US EPA, EPA/600/3-87/007, Athens,
559 GA.

560 FDEP 2006: Water Quality Credit Trading: A Report to the Governor and Legislature.
561 ([http://www.dep.state.fl.us/water/watersheds/docs/WQ_CreditTradingReport_fina](http://www.dep.state.fl.us/water/watersheds/docs/WQ_CreditTradingReport_final_December2006.pdf)
562 [l_December2006.pdf](http://www.dep.state.fl.us/water/watersheds/docs/WQ_CreditTradingReport_final_December2006.pdf), Feb/2013)

563 FDEP 2010: The Pilot Water Quality Credit Trading Program for the Lower St. Johns
564 River: A Report to the Governor and Legislature
565 ([http://www.dep.state.fl.us/water/wqssp/docs/WaterQualityCreditReport-](http://www.dep.state.fl.us/water/wqssp/docs/WaterQualityCreditReport-101410.pdf)
566 [101410.pdf](http://www.dep.state.fl.us/water/wqssp/docs/WaterQualityCreditReport-101410.pdf), Feb/2013).

567 FDEP 2012: Development of Numeric Nutrient Criteria for Florida Lakes, Spring Vents
568 and Streams ([http://www.dep.state.fl.us/water/wqssp/nutrients/docs/tsd-nnc-lakes-](http://www.dep.state.fl.us/water/wqssp/nutrients/docs/tsd-nnc-lakes-springs-streams.pdf)
569 [springs-streams.pdf](http://www.dep.state.fl.us/water/wqssp/nutrients/docs/tsd-nnc-lakes-springs-streams.pdf), Feb/2013).

570 Fernandez, GP., Chescheir, GM., Skaggs, RW., Amatya, DM. 2006: DRAINMOD-GIS:
571 a lumped parameter watershed scale drainage and water quality model. *Agr Water*
572 *Manage.* 81: 77–97

573 Franz, K. J., H. C. Hartmann, S. Sorooshian, and R. Bales. 2003: Verification of National
574 Weather Service ensemble streamflow predictions for water supply forecasting in
575 the Colorado River basin. *J. Hydrometeor.* 4: 1105–1118.

576 Gent PR, G Danabasoglu, LJ Donner, et al. 2011: The Community Climate System
577 Model Version 4. *J Climate.* 24: 4973-4991

578 Georgakakos, K. P., Seo, D.-J., Gupta, H., Schaake, J., and Butts, M. B. 2004:
579 Characterizing streamflow simulation uncertainty through multimodel ensembles,
580 *J. Hydrol.*, 298, 222–241

581 Higgins RW, Shi W, Yarosh E, Joyce R. 2000: Improved United States precipitation
582 quality control system and analysis. NCEP/ CPC ATLAS No. 7. Also available at:
583 http://www.cpc.ncep.noaa.gov/research_papers/ncep_cpc_atlas/7/index.html

584 Hirsch, R. M., Moyer, D. L. and Archfield, S. A. 2010: Weighted Regressions on Time,
585 Discharge, and Season (WRTDS), with an Application to Chesapeake Bay River
586 Inputs. *J Am Water Resour As.* 46: 857–880. doi: 10.1111/j.1752-
587 1688.2010.00482.x

588 Johanson, R.C., Imhoff, J.C., Davis, H.H., Kittle, J.L., Donigian, A.S. 1981: User's
589 Manual for Hydrologic Simulation Program-Fortran (HSPF), Release 7.0, US-
590 EPA, Athens, GA.

591 Kiladis GN, Diaz HF. 1989: Global climate extremes associated with extremes of the
592 Southern oscillation. *J Climate*. 2:1069–1090

593 Kirtman, B. P. and D. Min. 2009: Multimodel Ensemble ENSO prediction with CCSM
594 and CFS. *Mon. Wea. Rev.*137: 2908-2930.

595 Kirtman, B.P. et al. 2014: The North American Multi-Model Ensemble (NMME): Phase-
596 1 Seasonal to Interannual Prediction, Phase-2 Toward Developing Intra-Seasonal
597 Prediction. *Bull. Amer. Meteor. Soc.*, doi: 10.1175/BAMS-D-12-00050.1

598 Krishnamurti,T.N., Kishtawal,C.M., LaRow,T., Bachiochi,D., Zhang,Z, Williford,E.,
599 Gadgil,S. and Surendran,S. 1999: Improved weather and seasonal climate
600 forecasts from multimodel superensemble. *Science*. 285 No 5433: 1548-1550.

601 Kuczera, G. 1997: Efficient subspace probabilistic parameter optimization for catchment
602 models. *Water resour res.* 33(1): 177–185.

603 Kumar, A., and M. P. Hoerling, M. Ji, A. Leetmaa, and P. D. Sardeshmukh, 1996:
604 Assessing a GCM's suitability for making seasonal predictions. *J Climate*. 9:
605 115–129.

606 Li H and Misra V. 2013: Global Seasonal Climate Predictability in a Two Tiered
607 Forecast System. Part II: Boreal winter and spring seasons. *Clim Dynam.*
608 Available from
609 http://floridaclimateinstitute.org/images/document_library/publications/fish50-
610 [paper-partII-final.pdf](http://floridaclimateinstitute.org/images/document_library/publications/fish50-paper-partII-final.pdf)

611 Li, H., Sheffield, J., and Wood, E. F. 2010: Bias correction of monthly precipitation and
612 temperature fields from Intergovernmental Panel on Climate Change AR4 models
613 using equidistant quantile matching. *J Geophys Res.* 115, D10101,
614 doi:10.1029/2009jd012882.

615 Madsen H. 2000: Automatic calibration of a conceptual rainfall–runoff model using
616 multiple objectives. *J Hydrol.* 235: 276–288.

617 Marzban, C. 2004. The ROC Curve and the Area under It as Performance Measures.
618 *Wea. Forecasting*, 19: 1106–1114. doi: <http://dx.doi.org/10.1175/825.1>

619 Maurer, E.P., D.P. Lettenmaier, and N. J. Mantua. 2004: Variability and predictability of
620 North American runoff. *Water resour res.* 40(9), W09306
621 doi:10.1029/2003WR002789.

622 Misra V, Li H, Wu Z, DiNapoli S. 2013: Global seasonal climate predictability in a two
623 tiered forecast system. Part I: Boreal summer and fall seasons. *Clim Dyn.*
624 doi:10.1007/s00382-013-1812-y

625 NRC 2000: Clean Coastal Waters. National Academy Press, Washington, D.C

626 Obeysekera JA, Trimble P, Cadavid L, Santee R, White C. 1999: Use of Climate Outlook
627 for Water Management in South Florida, USA. South Florida Water Management
628 District: West Palm Beach, FL

629 Oh, J., and Sankarasubramanian A. 2012: Climate, Streamflow and Water Quality
630 Interactions over the Southeastern US, *Hydrol Earth Syst Sc.* 17: 2285-2298.

631 Palmer, T. N, C. Brankovic, and D. S. Richardson, 2000: A probability and decision
632 model analysis of PROVOST seasonal multi-model ensemble integrations. *Quart.*
633 *J. Roy. Meteor. Soc.*, 126, 2013-2034.

634 Pagano, T. C., D. C. Garen, T. R. Perkins, and P. A. Pasteris. 2009: Daily updating of
635 operational statistical seasonal water supply forecasts for the western US, *J Am*
636 *Water Resour As.* 45(3): 767–778.

637 Pagano, T. C., H. C. Hartmann, and S. Sorooshian, 2001: Using climate forecasts for
638 water management: Arizona and the 1997-2001 El Niño. *J Am Water Resour As.*
639 37: 1139–1153.

640 Palmer, T. N., Alessandri, A., Andersen, U. et al. 2004: Development of a European
641 multimodel ensemble system for seasonal to interannual prediction (DEMETER).
642 *Bull. Amer. Meteor. Soc.*85: 853-872.

643 Preston SD, Alexander RB, Schwarz GE, Crawford CG. 2011: Factors Affecting Stream
644 Nutrient Loads: A Synthesis of Regional SPARROW Model Results for the
645 Continental United States. *J Am Water Resour As.* 47(5): 891-915. doi:
646 10.1111/j.1752-1688.2011.00577.x.

647 Prudhomme, C., and H. Davies. 2009: Assessing uncertainties in climate change impact
648 analyses on the river flow regimes in the UK. Part 1: Baseline climate. *Climatic*
649 *Change.* 93: 177–195.

650 Ropelewski CF, Halpert MS. 1986: North American precipitation and temperature
651 patterns associated with the El Nino/Southern Oscillation (ENSO). *Monthly*
652 *Weather Review.* 114:2352–2362

653 Ropelewski CF, Halpert MS. 1987: Global and regional scale precipitation patterns
654 associated with the El Niño/Southern Oscillation. *Mon. Wea. Rev.*115:1606–
655 1626

656

657 Rosenberg, E. A., A. W. Wood, and A. C. Steinemann. 2011: Statistical applications of
658 physically based hydrologic models to seasonal streamflow forecasts. *Water*
659 *resour res.* 47, W00H14, doi:10.1029/2010WR010101.

660 Runkel, R.L., Crawford, C.G., and Cohn, T.A. 2004: Load Estimator (LOADEST): A
661 FORTRAN Program for Estimating Constituent Loads in Streams and Rivers:
662 U.S. Geological Survey Techniques and Methods Book 4, Chapter A5, 69 p.

663 Saha, S., and co-authors, 2010: The NCEP Climate Forecast Reanalysis. *Bull. Amer.*
664 *Meteor. Soc.* 91: 1015-1057.

665 Sankarasubramanian, A., Vogel, R.M., Limbrunner, J.F. 2001: The climate elasticity of
666 streamflow in the United States. *Water resour res.* 37(6): 1771-1781

667 Schaake, J., Cong, S., and Duan, Q. 2006: U.S Mopex Datasets, IAHS publication series
668 (<https://e-reports-ext.llnl.gov/pdf/333681.pdf>).

669 Shrestha, S., Kazama, F., Newham, LTH. 2008: A framework for estimating pollutant
670 export coefficients from long-term in-stream water quality monitoring data.
671 *Environ Modell Softw.* 23:182–194

672 Smith, R.A., Schwarz, G.E., Alexander, R.B. 1997: Regional Interpretation of water-
673 quality monitoring data. *Water resour res.* . 33 (12), 2781–2798.

674 Sugawara M. 1995: Tank model. In: Singh VP, editor. *Computer models of watershed*
675 *hydrology.* Littleton, Co.: Water Res. Publ., pp 165–214.

676 USEPA 2006: Reassessment of Point Source Nutrient Mass Loadings to the Mississippi
677 River Basin, November, 2006, Mississippi River/Gulf of Mexico Watershed
678 Nutrient Task Force. 2006a pp.

679 Wilks, D. S., 2001: A skill score based on economic value for probability
680 forecasts. *Meteor. Appl.*, 8, 209–219.

681 Wood A. W., Leung LR, Sridhar V, Lettenmaier DP. 2004: Hydrologic implications of
682 dynamical and statistical approaches to downscaling climate model outputs.
683 *Climatic Change*. 62: 189–216.

684 Wood, A. W., A. Kumar, and D. P. Lettenmaier. 2005: A retrospective assessment of
685 National Centers for Environmental Prediction climate model–based ensemble
686 hydrologic forecasting in the western United States. *J Geophys Res*. 110, D04105,
687 doi:10.1029/2004JD004508.

688 Wood, A. W., and Lettenmaier, D.P. 2006: A test bed for new seasonal hydrologic
689 forecasting approaches in the western United States. *Bull. Amer. Meteor. Soc.* 87:
690 1699–1712

691 Wood, A. W., John C. Schaake, 2008: Correcting Errors in Streamflow Forecast
692 Ensemble Mean and Spread. *J. Hydrometeor.* 9, 132–148.
693 doi: <http://dx.doi.org/10.1175/2007JHM862.1>
694

695 Yang, S. -C., C. Keppenne, M. Rienecker, E. Kalnay, 2009: Application of coupled bred
696 vectors to seasonal-to-interannual forecasting and ocean data assimilation. *J*
697 *Climate*. 22: 2850-2870.

698 Yao, H, and A. P. Georgakakos, 2001: Assessment of Folsom Lake Response to
699 Historical and Potential Future Climate Scenarios. *J Hydrol*. 249, 176-196.

700 Zhang, S., M.J. Harrison, A. Rosati, and A. Wittenberg, 2007: System design and
701 evaluation of coupled ensemble data assimilation for global oceanic studies. *Mon.*
702 *Wea. Rev.*. 135:3541–3564.
703
704
705

706 **List of Figures**

707

708 Fig. 1. Schematic of hydrological simulation based on multiple ensembles of climate
709 model forecasted meteorological forcing (60 members per seasonal forecast) and multiple
710 hydrological models (3 models), for a total of 180 seasonal hydrological simulations per
711 season per watershed.

712

713 Fig. 2. Climatological rainfall averaged over the 28 watersheds in the Southeastern U.S.
714 (identifiers indicated along the x-axis).

715

716 Fig. 3. Volume error of the flow predicted with forcing from raw FISH50 data (FISH50),
717 resampled from historical observational analogues of Dec-May mean rainfall from
718 FISH50 (FISH50_Resamp).

719

720 Fig. 4. Predicted monthly mean flow with raw FISH50 (FISH50), resampled from
721 historical observational analogues of Dec-May mean rainfall from FISH50
722 (FISH50_Resamp) forcing.

723

724 Fig. 5. Skill scores of the hydrological prediction based on normalized root mean square
725 errors. PEM (persistence efficiency measure) is the Nash Sutcliffe efficiency criteria
726 measured with respect to lag one-year as a reference forecast and NSE is the Nash
727 Sutcliffe efficiency measured with respect to climatological value as a reference forecast.

728

729 Fig. 6. Area under ROC (AROC) for FISH50 Dec–May mean precipitation averaged over
730 the respective watersheds in the Southeastern U.S. (a) AROC value for very wet (blue
731 circle) and very dry (red circle) rainfall categories, (b) AROC value for medium wet
732 (blue) and medium dry (red) categories. Only AROC values over 0.5 are shown. The size
733 of the bubble indicates the relative magnitude of the AROC, which can range from 0.5 to
734 1.0.

735

736 Fig. 7. Summary of probabilistic assessment of flow predicted with FISH50_Resamp for
737 four selected quartile categories of December-May mean rainfall over the various
738 watersheds in the Southeastern U.S (Very Dry, Very Wet, Medium Wet, and Medium
739 Dry). An AROC greater than 0.5 suggests that the prediction skill is better than the
740 climatology.

741

742 Fig. 8. AROC for the very wet (blue) and very dry (red) categories of streamflow
743 predicted with FISH50_Resamp forcing. The size of the bubble indicates the relative
744 magnitude of the AROC, which can range from 0.5 to 1.0. Values of AROC below 0.5
745 are not plotted.

746

747 Fig. 9. Same as Fig. 8 but for AROC values for the medium wet (blue) and medium dry
748 (red) categories of streamflow.

749

750 Fig. 10. AROC value for simulated (a) total nitrogen (upper quartile) and (b) total
751 phosphorous (upper quartile). Size of the blue circle represents the skill (AROC) of
752 streamflow and size of the red circle represents the skill of nutrient loading.

753

754 Fig. 11. AROC value for simulated (a) total nitrogen (lower quartile) and (b) total
755 phosphorous (lower quartile). Size of the blue circle represents the skill (AROC) of
756 streamflow and size of the red circle represents the skill of nutrient loading.

757

758 List of Tables

759

760 Table 1 General characteristics of the selected watershed

761 Table 2. Parameters and corresponding performance of nutrient loading rating curve
762 developed using LOADEST.

763

764

765

766

767

Table 1 General characteristics of the selected watershed

SN	Basin (USGS ID)	Lon	Lat	Area (Sq mile)	Annual Rain (mm)	Annual Ave runoff (Cumeecs)	River system
1	2456500	-87.0	33.7	885	1425	45.6	LOCUST FORK AT SAYRE, AL.
2	3574500	-86.3	34.6	320	1467	17.3	PAINT ROCK RIVER NEAR WOODVILLE AL
3	2414500	-85.6	33.1	1675	1425	86.3	TALLAPOOSA RIVER AT WADLEY AL
4	2296750	-81.9	27.2	1367	1248	44.8	PEACE RIVER AT ARCADIA, FLA.
5	2329000	-84.4	30.6	1140	1349	49.3	OCHLOCKONEE RIVER NR HAVANA, FLA.
6	2365500	-85.8	30.8	3499	1425	171.9	CHOCTAWHATCHEE RIVER AT CARYVILLE, FLA.
7	2375500	-87.2	31.0	3817	1493	201.2	ESCAMBIA RIVER NEAR CENTURY, FL
8	2236000	-81.4	29.0	3066	1293	97.7	ST. JOHNS RIVER NR DELAND, FLA.
9	2192000	-82.8	34.0	1430	1333	65.7	BROAD RIVER NEAR BELL, GA.
10	2202500	-81.4	32.2	2650	1189	85.4	OGEECHEE RIVER NEAR EDEN, GA.
11	2217500	-83.4	33.9	392	1385	19.9	MIDDLE OCONEE RIVER NEAR ATHENS, GA.
12	2347500	-84.2	32.7	1850	1317	78	FLINT RIVER NEAR CULLODEN, GA.
13	2383500	-84.8	34.6	831	1528	48	COOSAWATTEE RIVER NEAR PINE CHAPEL, GA.
14	2339500	-85.2	32.9	3550	1475	189.3	CHATTAHOOCHEE RIVER AT WEST POINT, GA.
15	2387000	-84.9	34.7	687	1433	37.2	CONASAUGA RIVER AT TILTON, GA.
16	2387500	-84.9	34.6	1602	1480	87.6	OOSTANAULA RIVER AT RESACA, GA.
17	2102000	-79.1	35.6	1434	1171	51	DEEP RIVER AT MONCURE, N.C.
18	2118000	-80.7	35.8	306	1257	13.9	SOUTH YADKIN RIVER NEAR MOCKSVILLE N C
19	2126000	-80.2	35.1	1372	1173	48.9	ROCKY RIVER NEAR NORWOOD, N. C.
20	2138500	-81.9	35.8	67	1436	4	LINVILLE RIVER NEAR NEBO N C
21	3443000	-82.6	35.3	296	2156	33.5	FRENCH BROAD RIVER AT BLANTYRE N C
22	3451500	-82.6	35.6	945	1544	70.7	FRENCH BROAD RIVER AT ASHEVILLE, N. C.
23	3504000	-83.6	35.1	52	1895	4.6	NANTAHALA RIVER NEAR RAINBOW SPRINGS, NC
24	3512000	-83.4	35.5	184	1720	14	OCONALUFTEE RIVER AT BIRDTOWN, N. C.
25	3550000	-84.0	35.1	104	1846	8.5	VALLEY RIVER AT TOMOTLA, N. C.
26	2156500	-81.4	34.6	2790	1319	139.1	BROAD RIVER NEAR CARLISLE, S. C.
27	2165000	-82.2	34.4	236	1340	10.6	REEDY RIVER NEAR WARE SHOALS,S.C.
28	3455000	-83.2	36.0	1858	1340	114.5	FRENCH BROAD RIVER NEAR NEWPORT, TN

Table 2. Parameters and corresponding performance of nutrient loading rating curve developed using LOADEST.

Sno	Nutrient	Station	No of data points	T'	Ln(Q)	a	a1	a2	a3	R ²	Mean Load (Ton/day)	SE
1	Total nitrogen	2296750	143	1984.77	6.30	7.76	1.04	0.17	0.13	0.90	4.89	0.30
2		2329000	133	1983.44	6.32	7.34	0.85	0.00	0.00	0.92	5.96	0.37
3		2365000	118	1983.52	8.82	9.07	0.93	-0.09	0.12	0.83	11.31	0.51
4		2375500	144	1983.14	8.61	8.87	1.04	0.12	-0.09	0.87	10.25	0.47
5		2236000	61	1985.65	7.41	8.55	1.11	-0.06	-0.06	0.90	10.69	0.58
6		2202500	141	1983.95	7.35	7.72	1.07	-0.08	-0.32	0.92	4.77	0.16
7		2126000	64	1984.76	7.25	8.92	1.08	-0.21	0.08	0.96	19.32	1.68
8	Total phosphorous	2296750	143	1984.77	6.30	7.60	0.75	-0.01	-0.02	0.72	3.09	0.13
9		2329000	133	1983.44	6.32	5.55	0.73	-0.03	0.03	0.82	0.81	0.07
10		2365000	118	1983.52	8.82	6.31	1.21	-0.02	0.11	0.82	0.77	0.06
11		2375500	144	1983.14	8.61	6.17	1.21	0.05	-0.10	0.85	0.80	0.09
12		2236000	61	1985.65	7.41	5.91	1.06	-0.15	0.22	0.80	0.84	0.11
13		2202500	141	1983.95	7.35	5.28	0.94	-0.13	-0.29	0.86	0.35	0.01
14		2126000	64	1984.76	7.25	6.95	1.03	-0.43	0.39	0.88	2.20	0.32

T' and Ln(Q)' are the centering parameter for time and log of flow

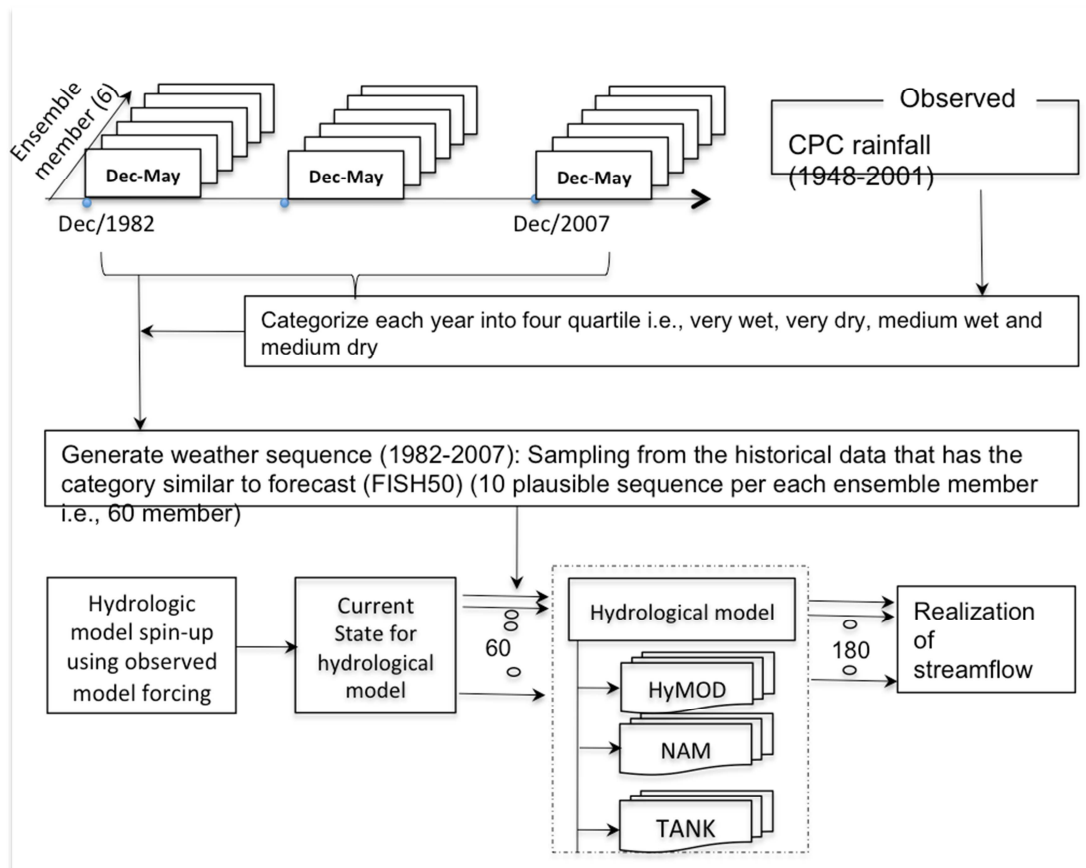


Fig. 1. Schematic of hydrological simulation based on multiple ensembles of climate model forecasted meteorological forcing (60 members per seasonal forecast) and multiple hydrological models (3 models), for a total of 180 seasonal hydrological simulations per season per watershed.

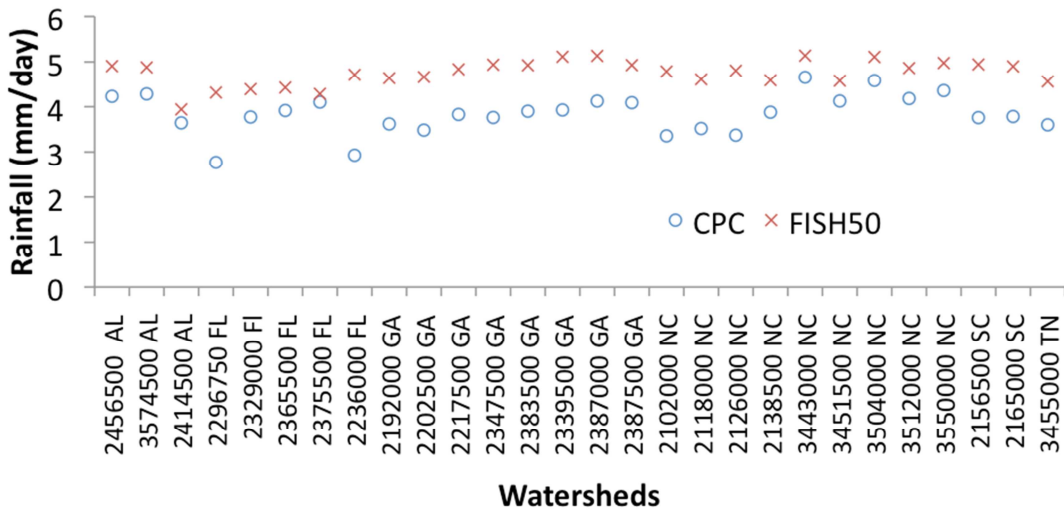


Fig. 2. Climatological rainfall averaged over the 28 watersheds in the Southeastern U.S. (identifiers indicated along the *x*-axis).

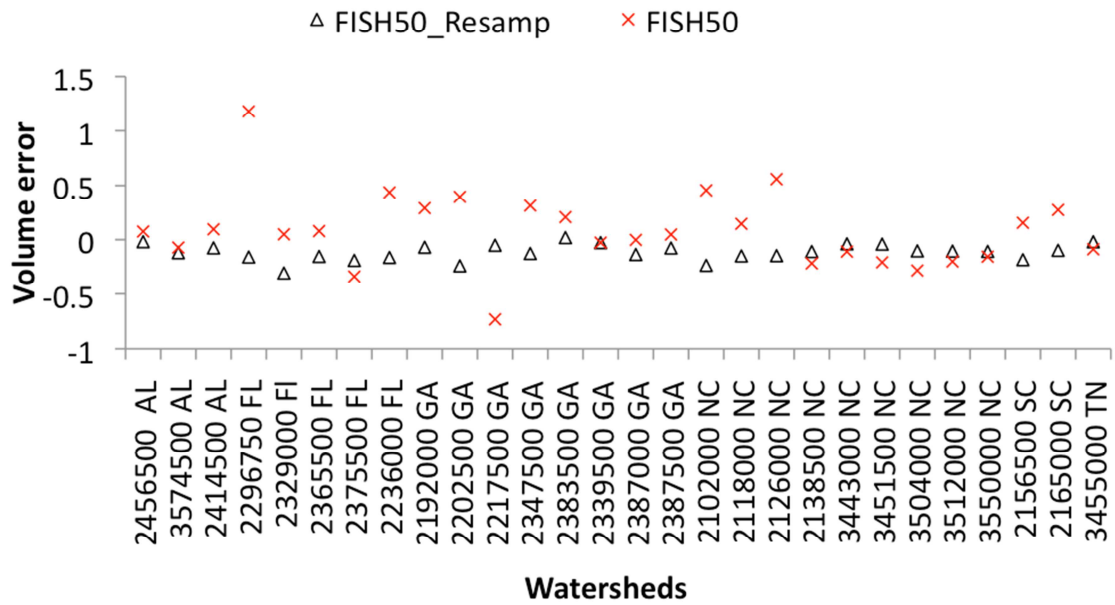


Fig. 3. Volume error of the flow predicted with forcing from raw FISH50 data (FISH50), resampled from historical observational analogues of Dec-May mean rainfall from FISH50 (FISH50_Resamp).

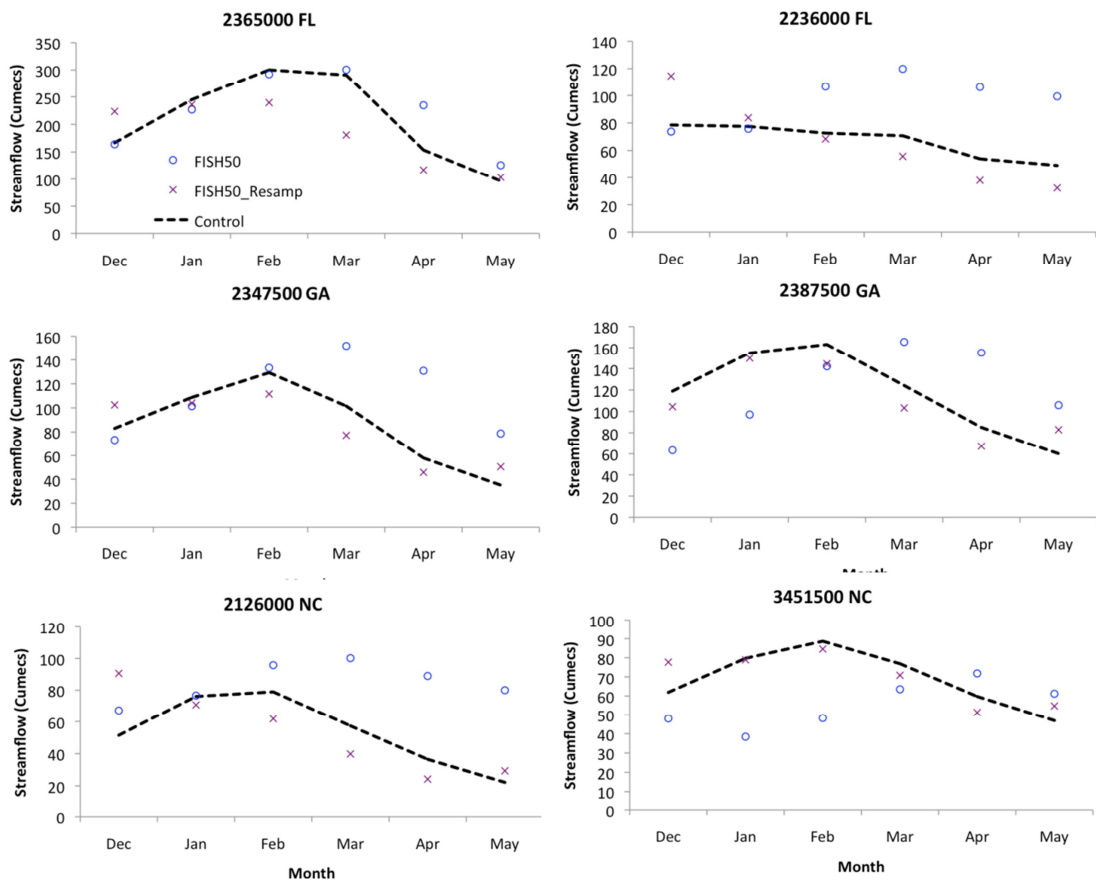


Fig. 4. Predicted monthly mean flow with raw FISH50 (FISH50), resampled from historical observational analogues of Dec-May mean rainfall from FISH50 (FISH50_Resamp) forcing.

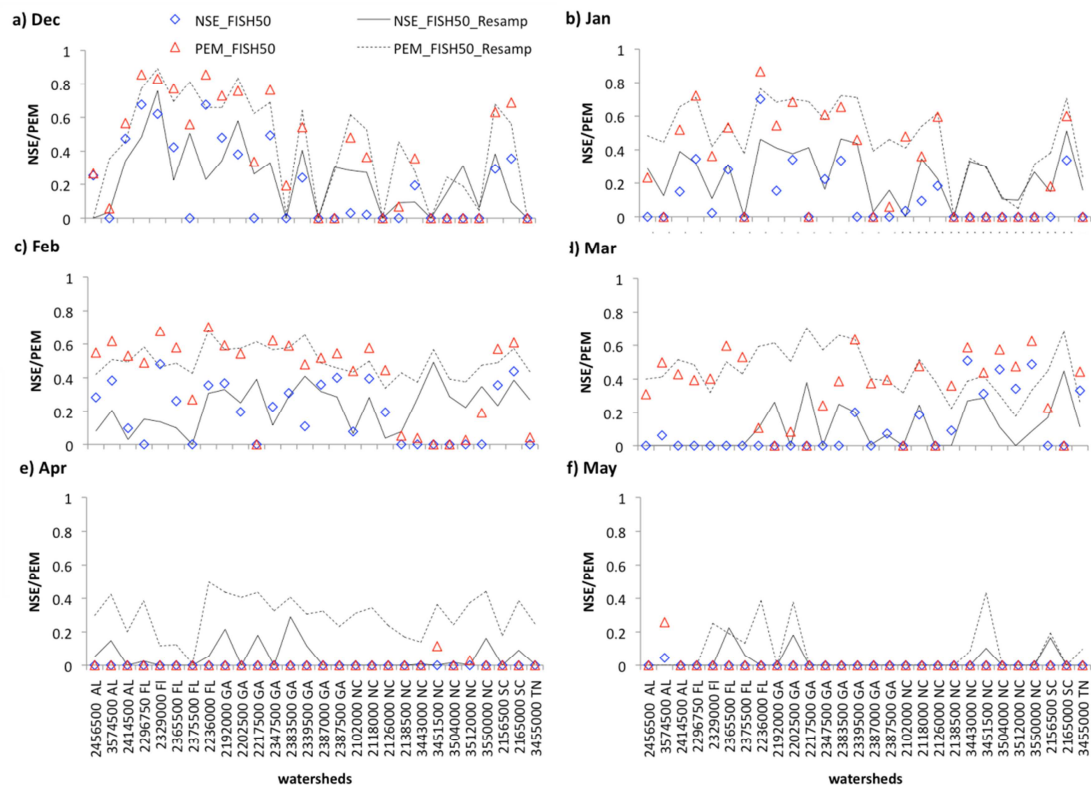


Fig. 5. Skill scores of the hydrological prediction based on normalized root mean square errors. PEM (persistence efficiency measure) is the Nash Sutcliffe efficiency criteria measured with respect to lag one-year as a reference forecast and NSE is the Nash Sutcliffe efficiency measured with respect to climatological value as a reference forecast.

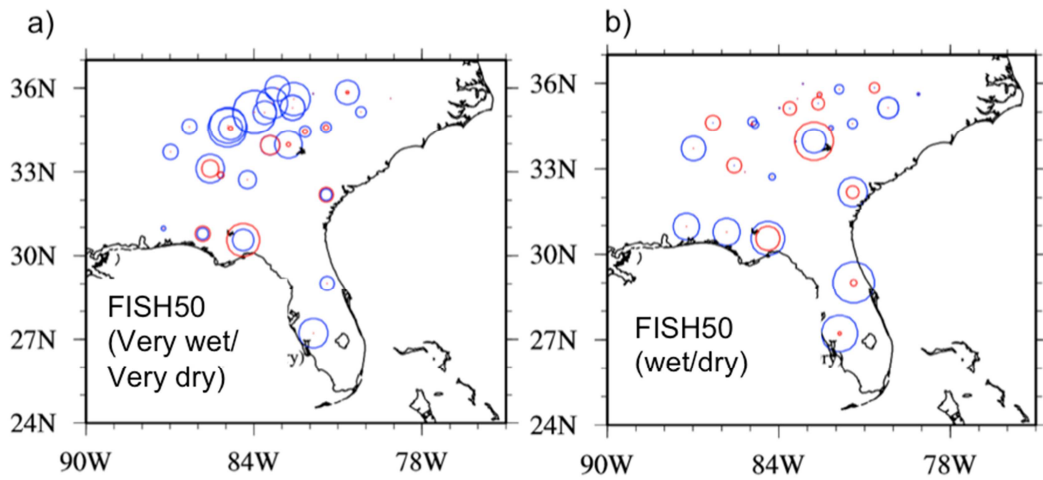


Fig. 6. Area under ROC (AROC) for FISH50 Dec–May mean precipitation averaged over the respective watersheds in the Southeastern U.S. (a) AROC value for very wet (blue circle) and very dry (red circle) rainfall categories, (b) AROC value for medium wet (blue) and medium dry (red) categories. Only AROC values over 0.5 are shown (for watershed with no skill, a dot is used to represent the location of the watershed). The size of the bubble indicates the relative magnitude of the AROC, which can range from 0.5 to 1.0.

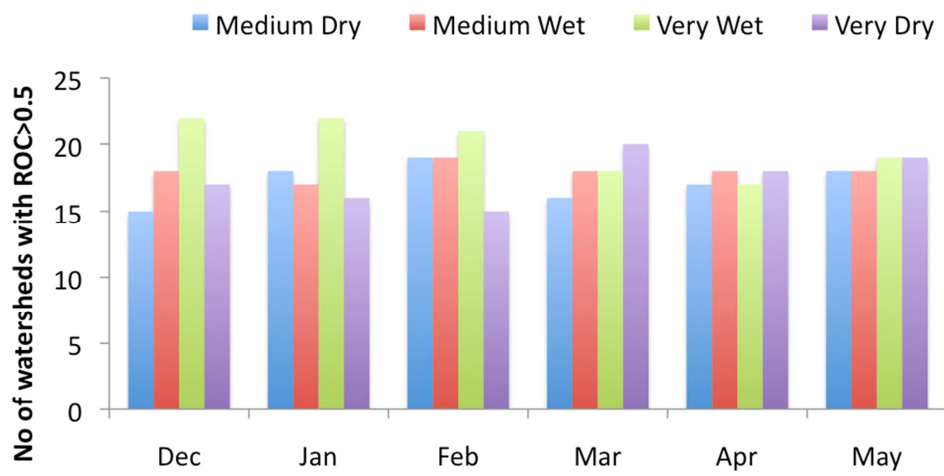


Fig. 7. Summary of probabilistic assessment of flow predicted with FISH50_Resamp for four selected quartile categories of December-May mean rainfall over the various watersheds in the Southeastern U.S (Very Dry, Very Wet, Medium Wet, and Medium Dry). An AROC greater than 0.5 suggests that the prediction skill is better than the climatology.

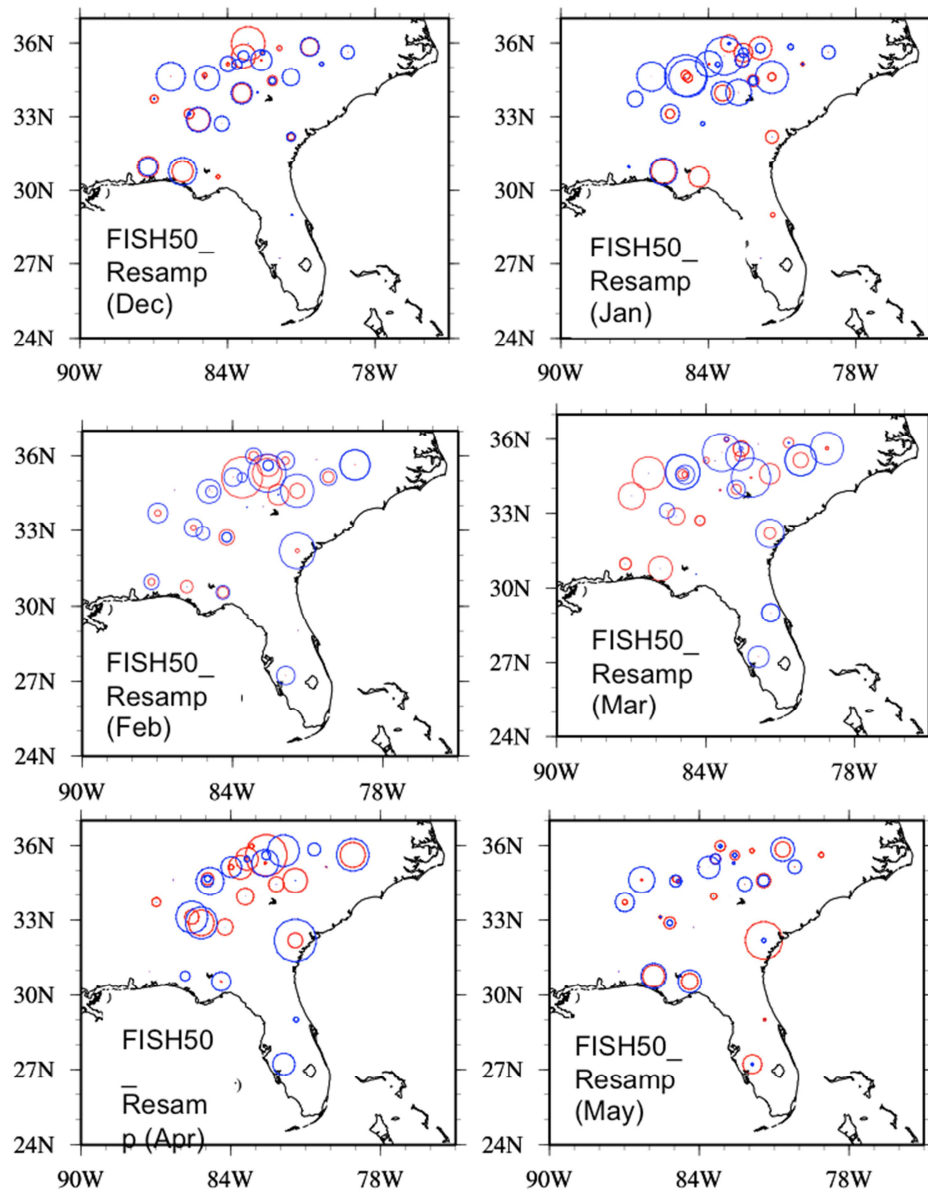


Fig. 8. AROC for the very wet (blue) and very dry (red) categories of streamflow predicted with FISH50_Resamp forcing. The size of the bubble indicates the relative magnitude of the AROC, which can range from 0.5 to 1.0. Values of AROC below 0.5 are not plotted.

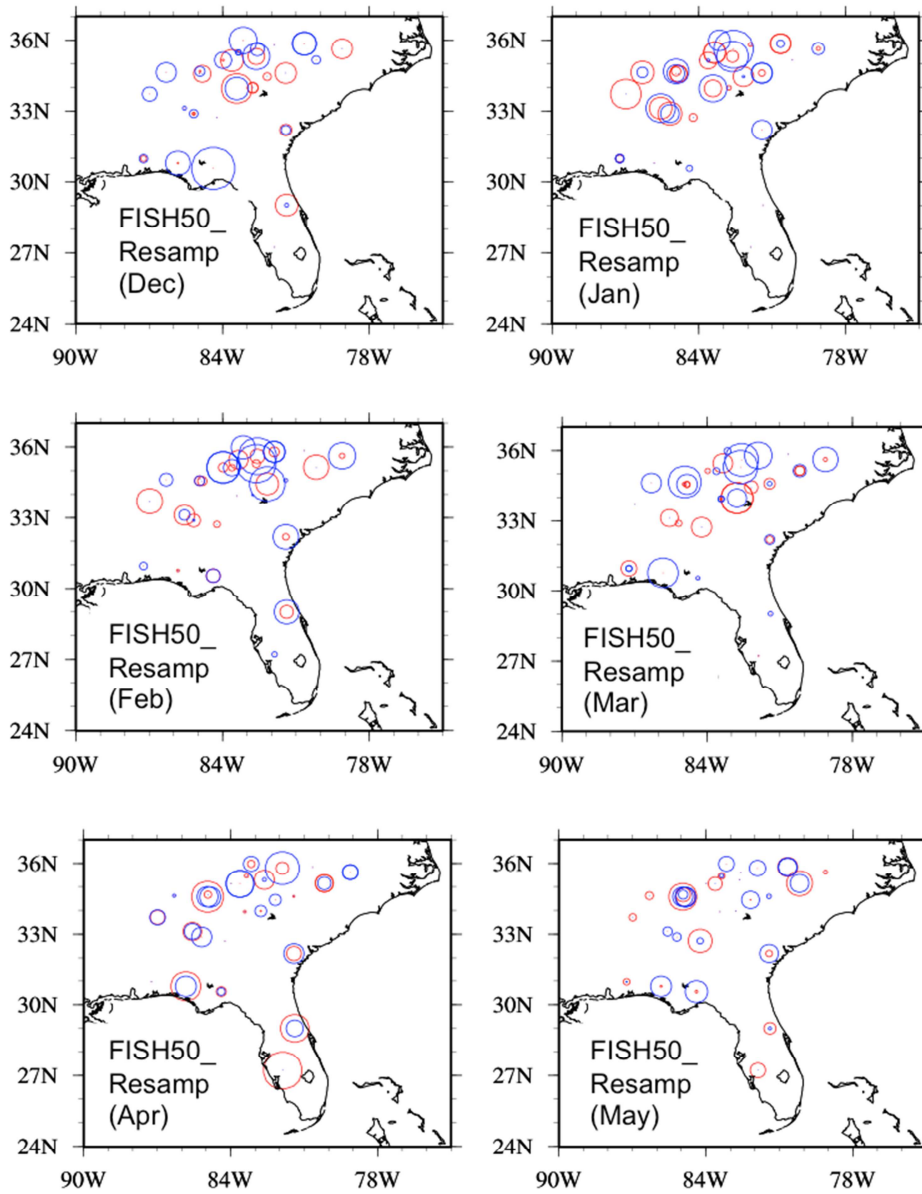


Fig. 9. Same as Fig. 9 but for AROC values for the medium wet (blue) and medium dry (red) categories of streamflow.

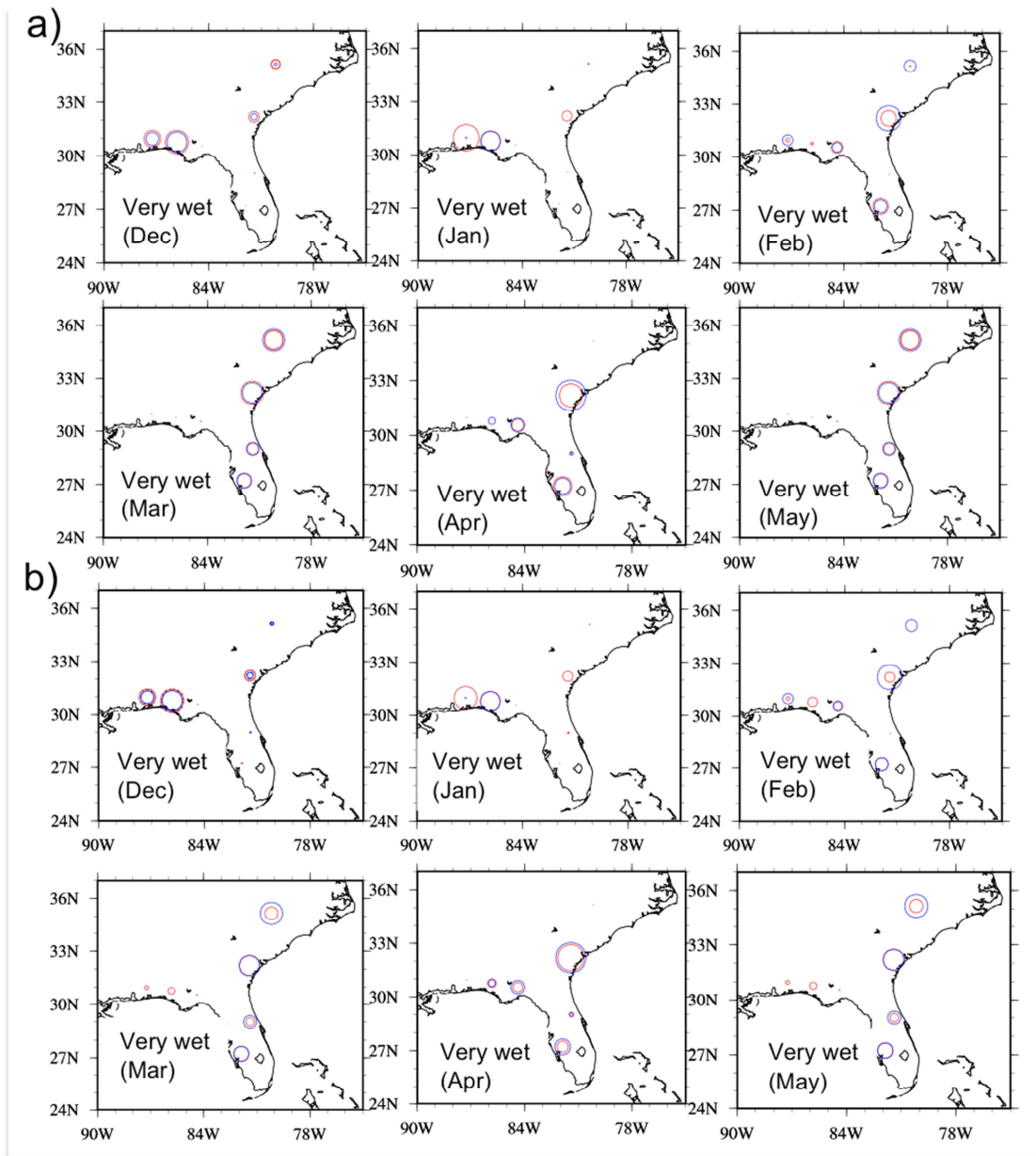


Fig. 10. AROC value for simulated (a) total nitrogen (upper quartile) and (b) total phosphorous (upper quartile). Size of the blue circle represents the skill (AROC) of streamflow and size of the red circle represents the skill of nutrient loading.

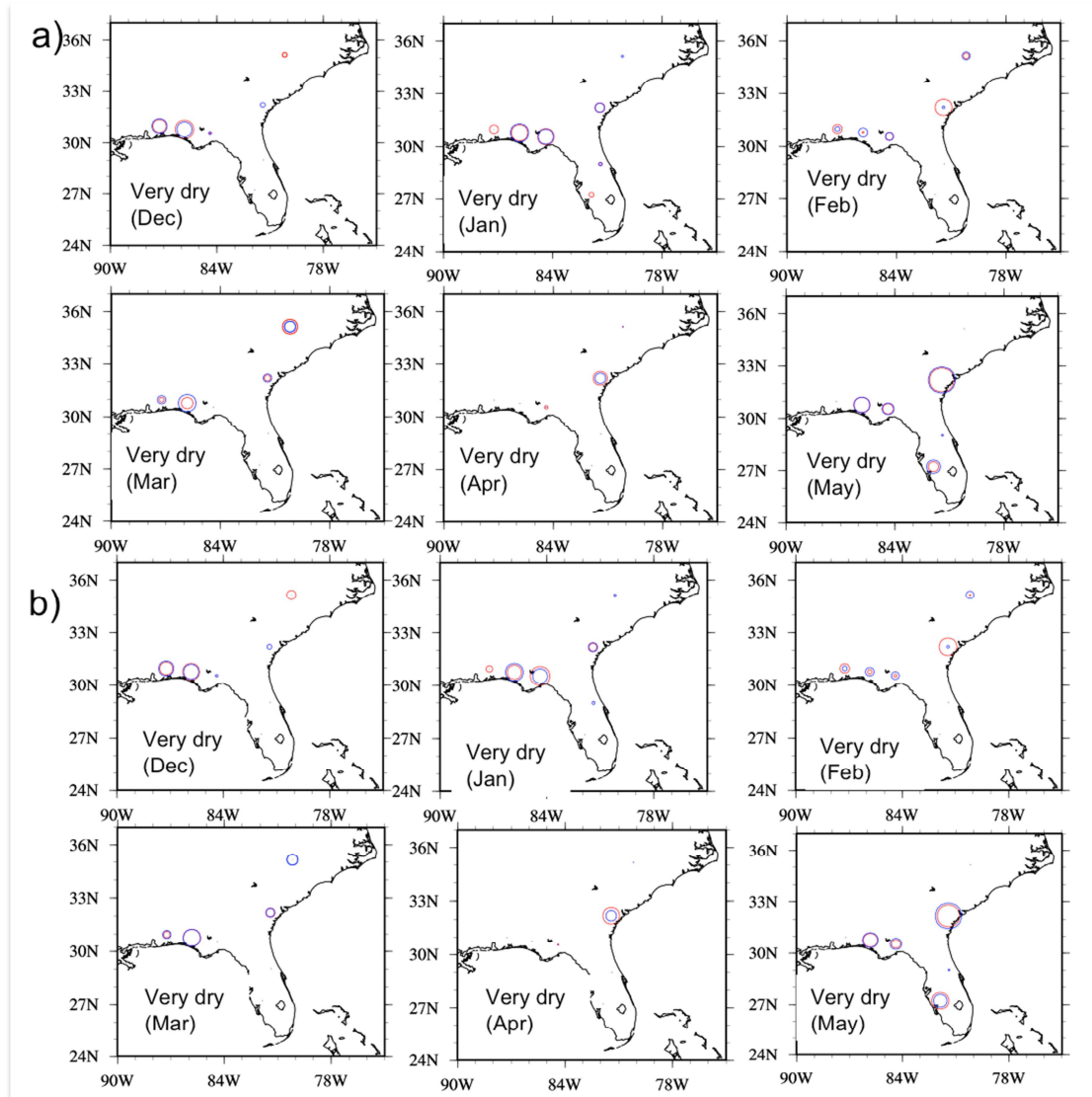


Figure 11: AROC value for simulated a) total nitrogen (lower quartile) and b) total phosphorous (lower quartile). Size of the blue circle represents the skill (AROC) of streamflow and red represents the skill of nutrient loading.